ChemPubSoc Europe

DOI: 10.1002/cptc.201900038

CHEMPHOTOCHEM Communications

Special Issue

Successive Photoswitching and Derivatization Effects in Photochromic Dithienylethene-Based Coordination Cages

Ru-Jin Li,[a] Muxin Han,[a] Jacopo Tessarolo,[a] Julian J. Holstein,[a] Jens Lübben,[b] Birger Dittrich,[c] Christian Volkmann,[b] Maik Finze,[d] Carsten Jenne,[e] and Guido H. Clever*[a]

A new series of $[Pd_2(\mathbf{L})_4]$ cages based on photochromic dithienylethene (DTE) ligands allowed us to gain insight into the successive photoswitching of multiple DTE moieties in a confined metallo-supramolecular assembly. Three new X-ray structures of $[Pd_2(o\text{-}\mathbf{L}^4)_4]$, $[Pd_2(o\text{-}\mathbf{L}^1)_2(c\text{-}\mathbf{L}^1)_2]$ and $[Pd_2(c\text{-}\mathbf{L}^1)_4]$ (o-**L** and c-**L** = open and closed forms of DTE ligands, respectively) were obtained. The structures deliver snapshots of three different combinations of DTE photoisomeric states within the cage, facilitating a comparison of the all-open with the all-closed, and most notably, an intermediate form where open and closed switches co-exist in the same cage. Moreover, a series of spherical anionic borate clusters was introduced in order to study their roles in the light-controllable host–guest chemistry. The binding guests show higher affinities with the flexible open cage $[Pd_2(o\text{-}\mathbf{L}^1)_4]$ than with the rigid closed cage $[Pd_2(c\text{-}\mathbf{L}^1)_4]$. For the $[B_{12}F_{12}]^{2-}$ guest, thermodynamic data obtained from NMR experiments was compared to results from isothermal titration calorimetry (ITC).

The synthesis of rationally designed and pre-functionalized self-assemblies represents one of the most vibrant topics in supramolecular chemistry.[1] The most complex architectures can undergo "smart" changes triggered by external stimuli (e.g. pH change, electrochemical inputs, temperature and light),[2] showing potential applications in chemical sensing,[3] biomedicine,[4] functional materials[5] as well as artificial molecular motors.[6] Therefore, the ability to precisely control state-switching events in supramolecular assemblies has been of uttermost interest in recent years.[7] Among the various examples of stimuli-responsive systems, light as a waste-free and non-invasive reagent, has been widely explored in supramolecular photochemistry.[8] A large amount of work describes light-switchable guest uptake and release,[9] photo-responsive catalysis,[10] light-triggered structural changes,[11] and photoresponsive supramolecular gels.[7c,12]

Among other photoactive compounds, dithienylethene (DTE) derivatives, owing to their formidable fatigue resistance, thermal irreversibility and, most important, their efficient and controllable photoswitching properties, have received significant attention.[13] Previously, we reported the self-assembly and light-triggered interconversion of $[Pd_2(o\text{-}\mathbf{L}^1)_4]$ and $[Pd_2(c\text{-}\mathbf{L}^1)_4]$ cages based on Pd^{II} ions and DTE-derived ligands, o-$\mathbf{L}^1$ (open photoisomeric form) and c-$\mathbf{L}^1$ (closed photoisomeric form), respectively.[9i] The interconversion between a structurally flexible $[Pd_2(o\text{-}\mathbf{L}^1)_4]$ cage and a rigid $[Pd_2(c\text{-}\mathbf{L}^1)_4]$ cage resulted in different binding affinities to the anionic guest $[B_{12}F_{12}]^{2-}$.

Mechanistic details regarding the switching of single photochromic DTE derivatives have been widely reported in the last decades.[14] However, for $[M_2L_4]$ metallosupramolecular architectures containing four DTE-based ligands, details concerning the course of consecutively converting all implemented switches remained still unclear. So far, it was not known whether open and closed ligand photoisomers can coexist in a single cage, if the switching of all four ligands occurs in an associated manner or if intermediate switching events are accompanied by decomplexation from the metal sites. In addition, we were interested in the effect of functionalization of guests and cages with further chemical moieties (e.g. solubilizing chains) on the performance of the system.

Herein, we report the synthesis of a series of DTE ligands based on $\mathbf{L}^1$ and corresponding self-assembled cages (Figure 1a and 1b). We found that the presence of different external substituents attached to the ligands does not interfere with neither the cage assembly nor the photoswitching properties. Furthermore, we show that the light-induced interconversion

[a] R.-J. Li, Dr. M. Han, Dr. J. Tessarolo, Dr. J. J. Holstein, Prof. Dr. G. H. Clever
Fakultät für Chemie und Chemische Biologie
Technische Universität Dortmund
Otto-Hahn-Straße 6, 44227 Dortmund (Germany)
E-mail: guido.clever@tu-dortmund.de
[b] Dr. J. Lübben, Dr. C. Volkmann
Institut für Anorganische Chemie
Georg-August-Universität Göttingen
Tammannstraße 4, 37077 Göttingen (Germany)
[c] Dr. B. Dittrich
Institut für Anorganische Chemie und Strukturchemie, Material- und Strukturforschung, Gebäude: 26.42
Heinrich-Heine Universität Düsseldorf
Universitätsstraße 1, 40225 Düsseldorf (Germany)
[d] Prof. Dr. M. Finze
Institut für Anorganische Chemie
Institut für nachhaltige Chemie and Katalyse mit Bor (ICB)
Julius-Maximilians-Universität Würzburg
Am Hubland, 97074 Würzburg (Germany)
[e] Prof. Dr. C. Jenne
Fakultät für Mathematik und Naturwissenschaften, Anorganische Chemie
Bergische Universität Wuppertal
Gaußstraße 20, 42119 Wuppertal (Germany)

Supporting information for this article is available on the WWW under https://doi.org/10.1002/cptc.201900038

An invited contribution to a Special Issue on Photoresponsive Molecular Switches and Machines

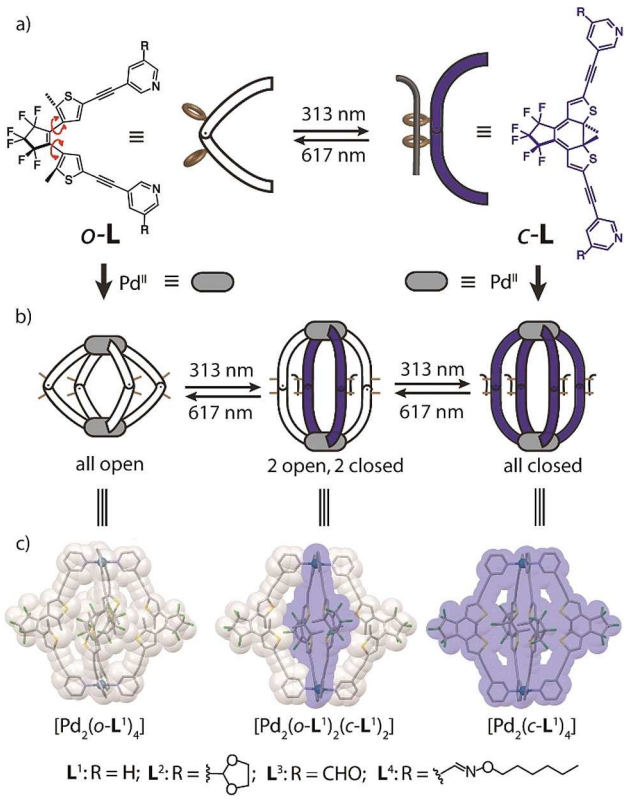

Figure 1. a) Reversible photo-switching of the dithienylethene-based ligands from open *o*-**L** form to closed *c*-**L** isomer; b) cartoon representations and c) X-ray structures illustrate the stepwise photochromic interconversion from (left) open cage [Pd$_2$(*o*-**L**^{1})$_4$] via several mixed-ligand intermediates, including (middle) *trans*-[Pd$_2$(*o*-**L**^{1})$_2$(*c*-**L**^{1})$_2$] with two open and two closed ligands, to (right) closed form cage [Pd$_2$(*c*-**L**^{1})$_4$].

between the all-open and all-closed photoisomeric forms of the cage proceeds stepwise *via* intermediates containing both the open- and the closed-form ligands, coexisting in a single cage assembly (Figure 1b–1c). We were able to obtain three new X-ray structures that showcase the initial, intermediate and end points of the photoswitching process. These structures allow one to compare the structural implications of the photoisomeric states that the ligands impart to the cage geometries.

Three new ligands, based on the previously reported **L**^{1} structure, were synthesized according to the following procedure. Ligand *o*-**L**^{2} was synthesized by a Sonogashira cross-coupling reaction of perfluoro-1,2-bis(2-iodo-5-methylthien-4-yl)cyclopentene and 3-(1,3-dioxolan-2-yl)-5-ethynylpyridine. Deprotection of the acetal afforded the aldehyde functionalized ligand *o*-**L**^{3}. Aldoxime ligand *o*-**L**^{4} was generated by the reaction of *O*-hexylhydroxylamine hydrochloride and aldehyde ligand *o*-**L**^{3} (Scheme S1, Supporting Information). The ligands can be reversibly interconverted between a conformationally flexible open form and a rigid closed-ring form by irradiation with UV light (313 nm) or light of 617 nm wavelength, respectively. For reasons of clarity, here only **L**^{3} is shown as an example. According to the ^{1}H NMR spectrum, the pale yellow *o*-**L**^{3} was converted into the intensely deep blue colored *c*-**L**^{3} isomer by irradiation at $\lambda = 313$ nm (in MeCN, yield $> 98\%$). The reverse

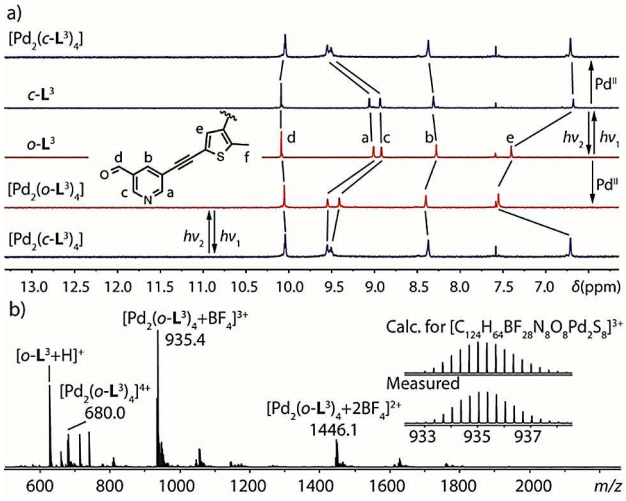

Figure 2. a) ^{1}H NMR spectra of ligands *o*-**L**^{3}, *c*-**L**^{3} and [Pd$_2$(*o*-**L**^{3})$_4$], [Pd$_2$(*c*-**L**^{3})$_4$] cages (300 MHz, CD_3CN, 293 K); b) ESI-MS spectrum of [Pd$_2$(*o*-**L**^{3})$_4$] cage.

isomerization proceeded quantitatively by irradiation at $\lambda =$ 617 nm (Figure 2). Upon formation of *c*-**L**^{3}, an upfield shift of the thiophene proton signal H_e was observed ($\Delta\delta = -0.72$ ppm). Additionally, the methyl proton signal H_f shifted downfield ($\Delta\delta = 0.20$ ppm; Figure S1, Supporting Information). By combining a 2:1 mixture of either ligand *o*-**L**^{3} or *c*-**L**^{3} with [Pd(CH$_3$CN)$_4$](BF$_4$)$_2$ in CD_3CN, the light yellowish cage complexes [Pd$_2$(*o*-**L**^{3})$_4$] and deep blue [Pd$_2$(*c*-**L**^{3})$_4$] were formed quantitatively. Assembly of the cages was observed by ^{1}H NMR spectroscopy (Figure 2). The proton signals of pyridine (H_{a-c}) and thiophene (H_e) rings of *o*-**L**^{3} were shifted downfield, whereas the aldehyde proton signal shifted slightly upfield upon complexation with the Pd^{II} ions. In the spectrum of [Pd$_2$(*c*-**L**^{3})$_4$], the protons H_a and H_c displayed remarkably similar downfield shifts, and the aldehyde proton H_d gave rise to a slight upfield shift. Both the pyridine proton H_b and thiophene proton H_e are shifted downfield. The stoichiometry of the [Pd$_2$(*o*-**L**^{3})$_4$] assembly was confirmed by electrospray ionization mass spectrometry (ESI-MS) (Figure 2b). For the formation of the [Pd$_2$(*o*-**L**^{3})$_4$] cage complex, the spectrum showed peaks corresponding to the [Pd$_2$(*o*-**L**^{3})$_4$]$^{4+}$, [Pd$_2$(*o*-**L**^{3})$_4$ + BF$_4$]$^{3+}$ and [Pd$_2$(*o*-**L**^{3})$_4$ + 2BF$_4$]$^{2+}$ species at $m/z = 680.0$, 935.4 and 1446.1 respectively. All peak patterns agreed with the calculated isotopic distributions.

In conformity with the photochemical behavior of the free ligand, the cage complexes showed similar properties. Both cage complexes [Pd$_2$(*o*-**L**^{3})$_4$] and [Pd$_2$(*c*-**L**^{3})$_4$] can be interconverted by irradiation with UV (313 nm) and red (617 nm) light, respectively. Before UV irradiation, strong absorption bands of *o*-**L**^{3} were observed below $\lambda_{max} = 400$ nm assignable to π–π^* transitions ($\lambda_{max} = 220$ and 312 nm for *o*-**L**^{3}, and $\lambda_{max} = 216$, 257 and 325 nm for [Pd$_2$(*o*-**L**^{3})$_4$]). Upon irradiation at 313 nm, new absorption bands were observed at $\lambda_{max} = 370$ and 602 nm for *c*-**L**^{3}, and at $\lambda_{max} = 395$ and 596 nm for [Pd$_2$(*c*-**L**^{3})$_4$]. Upon irradiation at 617 nm, the initial spectra were recovered, indicating that the ring-opening and closing processes are fully reversible (Figure 3).

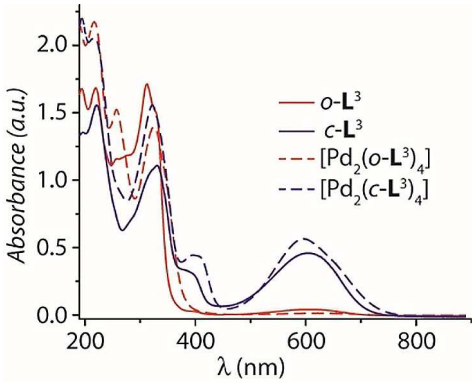

Figure 3. UV/Vis absorption spectra of *o*-L^3, *c*-L^3, $[Pd_2(o\text{-}L^3)_4]$ and $[Pd_2(c\text{-}L^3)_4]$.

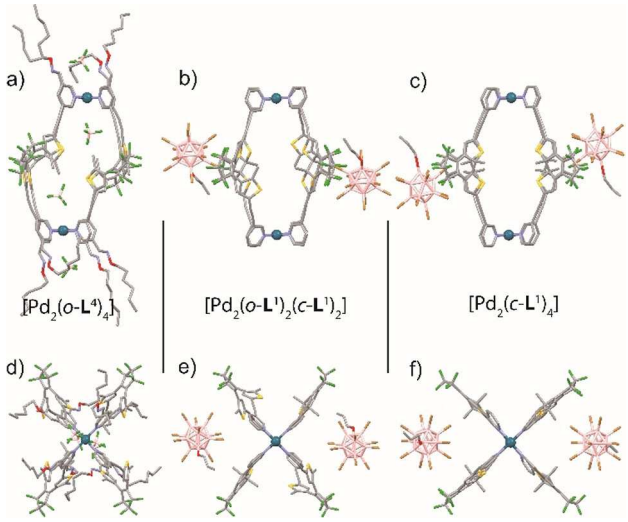

Figure 4. Three X-ray structures of DTE cages in different photoswitching states compared. a) Side view of flexible all-open cage $[Pd_2(o\text{-}L^4)_4]$ adopting an 'S' shape; b) intermediate-state cage $[Pd_2(o\text{-}L^1)_2(c\text{-}L^1)_2]$, and c) rigid all-closed cage $[Pd_2(c\text{-}L^1)_4]$. The top view of d) $[Pd_2(o\text{-}L^4)_4]$ shows that the counter anions BF_4^- sit close to the Pd–Pd axis inside the cavity. In contrast, propyl-oxy-functionalized spherical borate guests are positioned outside the cage boundaries in the solid-state structures of e) $[Pd_2(o\text{-}L^1)_2(c\text{-}L^1)_2]$, and f) $[Pd_2(c\text{-}L^1)_4]$. (C gray, N blue, O red, B pink, S yellow, F green, Br orange, Pd cyan-blue; solvent molecules and hydrogen atoms were omitted for clarity).

From the series of $[Pd_2(\mathbf{L})_4]$ (with $\mathbf{L}^{1,3,4}$) cages herein reported, three new crystal structures were obtained: i) $[Pd_2(o\text{-}L^4)_4]$, with all ligands in their open form; ii) $[Pd_2(o\text{-}L^1)_2(c\text{-}L^1)_2]$, with ligands coexisting in both open and closed forms; iii) $[Pd_2(c\text{-}L^1)_4]$ with all ligands in their closed form (Figure 4). In all three structures, parts of the DTE moieties, flexible ligand side chains, co-crystallized acetonitrile molecules, tetrafluoroborate counterions and boron clusters were found to be conformationally disordered over several positions. Hence, geometrical restraints for structural modelling and X-ray structure refinement had to be utilized (see Supporting Information). Single crystals of $[Pd_2(o\text{-}L^4)_4]$, suitable for single-crystal X-ray diffraction analysis, were obtained by slow evaporation of a 1 mM CD_3CN solution of the cage complex. Within the cage framework, each of the C_2-symmetric ligands can in principle adopt two enantiomeric forms (*P* and *M*). Even though six possible stereoisomers are theoretically conceivable for the cage,[9i] only the *PPMM* isomer of $[Pd_2(o\text{-}L^4)_4]$ was isolated in the solid state (Figure 4a and d). Previously, we demonstrated the coexistence (and interconversion) of all six possible stereoisomers of cage $[Pd_2(o\text{-}L^1)_4]$ in solution using in-depth NMR analyses and DFT geometry optimization studies. However, also that study revealed that only one stereoisomer (*PPMM meso*-form) of the cage $[Pd_2(o\text{-}L^1)_4]$ happened to crystallize as observed in its solid state structure.[9i] Here, $[Pd_2(o\text{-}L^4)_4]$ crystallized with half of the cage constituting the asymmetric unit. The entire structure suffers from severe disorder due to the conformational flexibility of the open-form ligand *o*-L^4 and the presence of alkyl side chains. Two tetrafluoroborate counterions were also modeled (shortest Pd–F distance is 3.04 Å). Interestingly, one of the two ligand positions in the asymmetric unit showed a slight degree of conversion to the closed-form ligand *c*-L^4. Specifically, refinement data shows two parts, the open-form ligand contributes for 85.0(3)% while the closed-form ligand contribute for 15.0(3)%. These results agree with the previously reported structure of the open cage $[Pd_2(o\text{-}L^1)_4]$, in which some residual density peaks deriving from the closed-form ligand were reported as well.[9i] The presence of partially photoswitched ligand can be explained with the difficulty to completely avoid light sources while handling, mounting and centering the crystal on the diffractometer. Single crystals of $[Pd_2(o\text{-}L^1)_2(c\text{-}L^1)_2]$ were obtained after slow evaporation (six months) from a CD_3CN solution of $[Pd_2(o\text{-}L^1)_4]$ with a chain-functionalized boron cluster $[(CH_3(CH_2)_2O)B_{12}Br_{11}]^{2-}$ (G12),[15] that was not found to enter the cage cavity (in accordance with the solution studies) but rather acts as a co-crystallization agent. Surprisingly, from the light yellowish solution of the $[Pd_2(o\text{-}L^1)_4]$ cage, a transparent blue single crystal was obtained. As the blue color is peculiar for the closed-form isomer, we suspect an unintended exposure to sunlight during crystal growth being responsible for at least a partial conversion of the open ligands to the closed form in the cage. The presence of a significant share of closed-form ligands was then confirmed by X-ray structural analysis. The cage crystallizes with one Pd^{II} ion and two ligands in the asymmetric unit. The DTE moiety of both ligands is disordered, however it was possible to model the structure splitting every backbone in two parts, one as an open-form and the other one as a closed-form ligand. Interestingly, in this case the contribution of *o*-L^1 and *c*-L^1 is almost the same in every ligand. Refined data shows for one ligand a contribution of 54.2(8)% for *o*-L^1 and 45.8(8)% for *c*-L^1, while for the second ligand the contribution is 59.5(6)% for *o*-L^1 and 40.5(8)% for *c*-L^1. Hence, X-ray results suggest a distribution of open- and closed-form ligands over all individual $[Pd_2(L^4)_4]$ units, meaning that the majority of cages represent a $[Pd_2(o\text{-}L^1)_2(c\text{-}L^1)_2]$ stoichiometry (with same photoisomers adopting a *trans* relationship for symmetry reasons). This unambiguously shows that open- and closed ligand photoisomers can co-exist as parts of the same cage structure (Figures 1c, 4b and e; as a simplification, we restricted depiction and discussion of this situation to the major isomer $[Pd_2(o\text{-}L^1)_2(c\text{-}L^1)_2]$). Finally, deep blue single crystals of $[Pd_2(c\text{-}L^1)_4]$ were obtained overnight from a CD_3CN solution of the closed-cage assemblies with

borate anion G12, again found to co-crystallize outside the cage boundaries. Also in this case, the system crystallizes with half of the cage in the asymmetric unit and with a disordered ligand-backbone. The latter situation, however, is caused by the statistical distribution of *R*,*R*- and *S*,*S*-enantiomers of completely closed-form ligand, exclusively (Supporting Information). Intriguingly, for both $[Pd_2(o\text{-}L^1)_2(c\text{-}L^1)_2]$ and $[Pd_2(c\text{-}L^1)_4]$ cage samples, we found that the boron cluster anion G12 was not encapsulated (Figure 4b and c). While we previously showed that $[B_{12}F_{12}]^{2-}$ (G1) is both encapsulated by $[Pd_2(o\text{-}L^1)_4]$ and $[Pd_2(c\text{-}L^1)_4]$ (albeit with low affinity for the second one), the herein studied alternative G12 does not bind in either cage isomer (Supporting Information). While initially suspecting the chain functionality of $[(CH_3(CH_2)_2O)B_{12}Br_{11}]^{2-}$ to abolish binding, subsequent titrations with $[B_{12}Br_{12}]^{2-}$ also showed no clear signs for guest uptake (similar for $[B_{12}Cl_{12}]^{2-}$ and many other borates, see Supporting Information).

The X-ray structures reveal cavities with a spherical void of diameter = 10.23 Å for $[Pd_2(o\text{-}L^1)_2(c\text{-}L^1)_2]$ and 9.42 Å for $[Pd_2(c\text{-}L^1)_4]$, filled with solvent molecules. Compared with $[Pd_2(o\text{-}L^4)_4]$, showing a void diameter of only 5.58 Å, the cages with, at least partially closed ligands possess a bigger inner pocket (void diameter was defined as maximum interatomic distance within the cavity, see Supporting Information, Figure S2). Looking at the three reported structures and the previously reported $[Pd_2(o\text{-}L^1)_4]$ assembly,[9i] it is possible to compare their shape to better understand the effect of the flexibility/rigidity of the open/closed ligands on the DTE-based self-assembled cages. The overall shape of open cage $[Pd_2(o\text{-}L^4)_4]$ with four flexible ligands shows an 'S' appearance in side view, skewed between two parallel {Pd(pyridine)$_4$} planes (Figure 4a). While rigid closed-form cage $[Pd_2(c\text{-}L^1)_4]$ and intermediate-state cage $[Pd_2(o\text{-}L^1)_2(c\text{-}L^1)_2]$ look relatively straight (with respect to the Pd–Pd axis) and more symmetric (Figure 4b and c). In the $[Pd_2(o\text{-}L^1)_2(c\text{-}L^1)_2]$ cage (Figure 4b), even though there are flexible ligands, the rigid ligands override and dictate the overall shape of the cage, imprinting their conformation on the flexible ligands. All cages were found to be closely packed sharing the same Pd–Pd axis direction. In $[Pd_2(o\text{-}L^4)_4]$, the assemblies are interacting with each other through close side chain contacts. Two alkyl chains are folding back towards the cage they are attached to, two are penetrating into the cavities of neighboring cages, contributing to the close packing of the system. For $[Pd_2(o\text{-}L^1)_2(c\text{-}L^1)_2]$, two adjacent cages are perpendicular to each other, and the Pd–Pd axes of these cages are packed in a zigzag-like orientation along the *c* axis. In the $[Pd_2(c\text{-}L^1)_4]$ structure, cages are in a close AB packing along the b axis, while the two Pd–Pd axes of cages in layers A and B are perpendicular to each other (Figure S3, Supporting Information).

The overall shape of the cages mainly arises from the DTE-ligands' conformational flexibility. Thus, we analyzed the ligand geometry within the cage confinement through three parameters: *i*) step angle (φ), measured as the angle between the Pd-Pd axis and the {Pd(pyridine)$_4$} planes; *ii*) offset distance, the minimum distance between the two normals from the two {Pd(pyridine)$_4$} planes passing through the corresponding Pd atom;

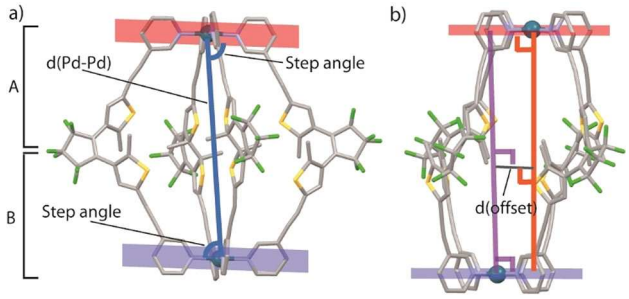

Figure 5. X-ray structure of $[Pd_2(o\text{-}L^1)_4]$ showing a) two halves (A and B) of the ligand arms in the cage, Pd–Pd distance, step angleφ, and b) offset distance.

iii) Pd–Pd distance, the distance between two Pd^{II} atoms in a cage (Figure 5). Firstly, by comparing the tilt degree of these cages, it is possible to notice that the open cage shows a greater inclination than the closed cage. The step angles for the open cages are 82.91° for $[Pd_2(o\text{-}L^1)_4]$ and 79.00° for $[Pd_2(o\text{-}L^4)_4]$, both smaller than that of closed cage $[Pd_2(c\text{-}L^1)_4]$ with 85.22° (Table 1). The offset distance can be used to explain the differences of flexible 'S' shape open cage and rigid closed-form cage. The obtained value for closed cage $[Pd_2(c\text{-}L^1)_4]$ is 1.47 Å, much shorter than that for open cages $[Pd_2(o\text{-}L^1)_4]$ (2.75 Å) and $[Pd_2(o\text{-}L^4)_4]$ (2.95 Å). Finally, comparison of the Pd-Pd distances reveals for rigid closed cage $[Pd_2(c\text{-}L^1)_4]$ a value of 15.92 Å, however, for the open cages $[Pd_2(o\text{-}L^1)_4]$ and $[Pd_2(o\text{-}L^4)_4]$ values of 16.52 Å and 15.63 Å, respectively, further indicating the structural flexibility of the open cage (Table 1). Regarding the intermediate-state cage $[Pd_2(o\text{-}L^1)_2(c\text{-}L^1)_2]$, its step angles, offset distance and Pd–Pd distance are very close to the fully closed cage $[Pd_2(c\text{-}L^1)_4]$, confirming that the contained rigid ligands determine the overall shape and dictate the rigidity of this structure.

On the basis of the differences in size and shape for the studied cages, we further investigated the binding abilities of the previously reported $[Pd_2(o\text{-}L^1)_4]$ and $[Pd_2(c\text{-}L^1)_4]$ assemblies towards a series of borate guests through NMR titrations (Supporting Information). Unfortunately, we could only calculate binding constants for $[B_{12}F_{12}]^{2-}$ (G1) and [1-H-*closo*-1-$CB_{11}F_{11}]^-$ (G3),[16] for both cages (Table S3, Supporting Information). Further guests were only found to bind to the open form cage (Supporting Information). Stepwise addition of G3 to $[Pd_2(o\text{-}L^1)_4]$ and $[Pd_2(c\text{-}L^1)_4]$, leads to significant signal shifts of the cage protons, particularly the inward-pointing H_a protons. We determined the association constants of the host-guest com-

Table 1. Comparison of relevant parameters of cages in X-ray crystal structures.

Crystal	d_{Pd-Pd} [Å][a]	d_{offset} [Å][b]	φ [°][c]
$[Pd_2(o\text{-}L^1)_4]$	16.52	2.75	82.91
$[Pd_2(o\text{-}L^4)_4]$	15.63	2.95	79.00
$[Pd_2(o\text{-}L^1)_2(c\text{-}L^1)_2]$	15.95	1.31	85.97
$[Pd_2(c\text{-}L^1)_4]$	15.99	1.47	85.22

[a] Pd–Pd distance; [b] Offset distance; [c] Step angle.

plexes from the titration data by non-linear regression methods (Table S3). The association constant K_a were estimated to be 258 M^{-1} for G3@[Pd_2(*o*-L^1)$_4$] and about 6 M^{-1} for G3@[Pd_2(*c*-L^1)$_4$] at 293 K (where binding in the last case was unambiguously indicated by an NMR shift but the very small value for K has to be taken with care). As observed before for G1, the open cage [Pd_2(*o*-L^1)$_4$] shows a stronger affinity for guest G3 than the closed cage [Pd_2(*c*-L^1)$_4$], but values turned out to be significantly lower in comparison to $[B_{12}F_{12}]^{2-}$ (G1) ($K_o = 3.2\times10^4$ M^{-1}; $K_c = 6.7\times10^2$ M^{-1}, obtained from NMR titration).[9i] We further evaluated the binding affinity between the [Pd_2(L^1)$_4$] cages and $[B_{12}F_{12}]^{2-}$ guest by isothermal titration calorimetry (ITC) (Figure 6b). From the analysis of calorimetric data at 298 K, a

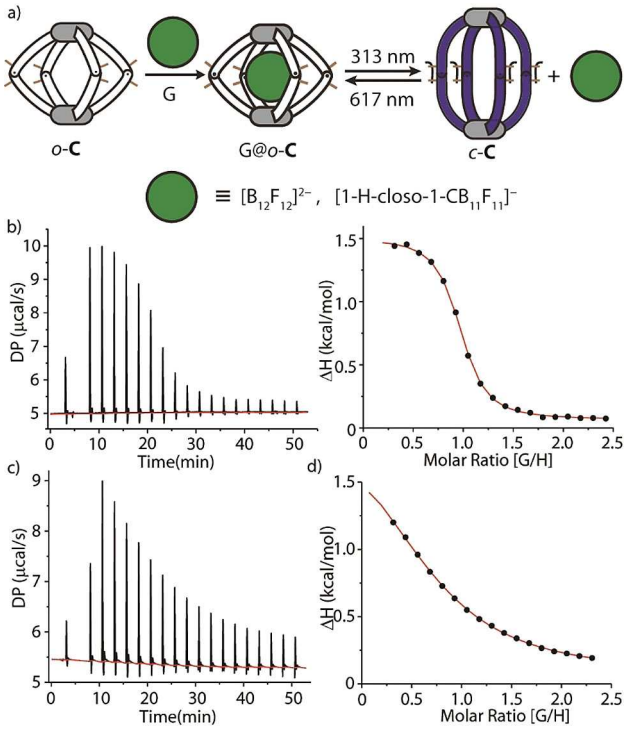

Figure 6. a) Schematic representation showing guest uptake and ejection triggered by irradiation at different wavelengths; isothermal titration calorimetry (ITC) data of b) [Pd_2(*o*-L^1)$_4$] and [Pd_2(*c*-L^1)$_4$] with the guest $[B_{12}F_{12}]^{2-}$ at 298 K.

binding constant of $K_o = 4.6\times10^4$ M^{-1} was obtained for G1@[Pd_2(*o*-L^1)$_4$] and $K_c = 2.1\times10^3$ M^{-1} for G1@[Pd_2(*c*-L^1)$_4$] (Supporting Information), thus delivering coherent results compared to the data obtained by NMR titration. Thermodynamic data obtained from ITC gave values of $\Delta S_{o\text{-}C} = 110$ $JK^{-1}mol^{-1}$ and $\Delta H_{o\text{-}C} =$ 6 $kJ\,mol^{-1}$ for the open cage host-guest binding, while $\Delta S_{c\text{-}C} =$ 95 $JK^{-1}mol^{-1}$ and $\Delta H_{c\text{-}C} = 10$ $kJ\,mol^{-1}$ were obtained for the closed cage. This data can be compared with the thermodynamic parameters obtained by NMR titration using the van't Hoff method with $\Delta S_{o\text{-}C} = 187$ $JK^{-1}mol^{-1}$ and $\Delta H_{o\text{-}C} =$ 30 $kJ\,mol^{-1}$ for the open cage, and $\Delta S_{c\text{-}C} = 56$ $JK^{-1}mol^{-1}$ $\Delta H_{c\text{-}C} =$ 0.6 $kJ\,mol^{-1}$ for the closed cage.[9i] Results obtained with both techniques agreed that the guest encapsulation process is entropy driven and favored for the open cage. This finding supports our previous assumption that differences in cavity solvation as well as structural flexibility of the cage framework play major roles in controlling guest affinity. While the free energy values of guest binding obtained by the two methods were found to agree quite well (open cage: −26.61 vs. −24.51, closed cage: −18.98 vs. −15.90 kJ/mol [ITC/NMR]), the extent of enthalpic and entropic contributions differ significantly (Supporting Information).

In conclusion, two externally functionalized cages [Pd_2(L^3)$_4$] and [Pd_2(L^4)$_4$] have been synthesized without encountering any influence on the fidelities of cage assembly and photoswitching. We obtained three new X-ray structures of [Pd_2(*o*-L^4)$_4$], [Pd_2(*o*-L^1)$_2$(*c*-L^1)$_2$] and [Pd_2(*c*-L^1)$_4$], which, together with a reported structure of [Pd_2(*o*-L^1)$_4$], exhibited different combinations of DTE photoisomeric states within each supramolecular assembly. These results highlight how the interconversion from open- to closed-form ligand in a self-assembled cage compound proceeds stepwise *via* intermediates. These findings are in agreement with our recent publication, in which we demonstrate the role of sequential DTE-backbone photoswitching in the guest release mechanism in related DTE-based supramolecular cages.[17] Detailed analysis of the herein reported structures through tilt angle, offset distance and Pd–Pd distance parameters allowed us to deepen the understanding of the photoswitching processes in a confined cage assembly. Finally, systematically studying light-switchable host-guest chemistry with a series of boron cluster guests confirmed the more flexible open-form [Pd_2(*o*-L^1)$_4$] to show the strongest guest affinity while derivatization of the best-binding guest $[B_{12}F_{12}]^{2-}$ (G1) was found to reduce or abolish encapsulation. The herein studied supramolecular systems containing multiple photoswitches have the potential to form the basis of stimuli-responsive receptors and light-triggered containers to release molecular cargo in various contexts, ranging from catalytic to medicinal applications. Furthermore, refined understanding of photoswitch interplay in complex architectures has relevance for research in the fields of nano-structured, intelligent materials and molecular machines.

Experimental Section

CCDC no 1456903, 1890769 and 1890770 contain the supplementary crystallographic data for [Pd_2(*o*-L^4)$_4$], [Pd_2(*o*-L^1)$_2$(*c*-L^1)$_2$] and [Pd_2(*c*-L^1)$_4$] first reported in this paper. These data can be obtained free of charge from The Cambridge Crystallographic Data Centre via www.ccdc.cam.ac.uk/data_request/cif.

Acknowledgements

We thank Dr. M. John (Georg-August Universität Göttingen) and Prof. Dr. W. Hiller (TU Dortmund) for help with NMR spectroscopy, Dr. H. Frauendorf (GAU Göttingen) for measuring the ESI-MS spectra, and Dr. M. D. Johnstone for help with the manuscript. We thank Prof. Dr. S. Schneider, Dr. C. Würtele and staff at the PXII (X06SA) beamline of the Swiss Light Source, Paul Scherrer Institut, Villigen, Switzerland for supporting the X-ray structure collection.

We thank the DFG under SFB 1073 (project B05), and GRK 2376 ('Confinement-controlled Chemistry'; 331085229), and the European Research Council (ERC Consolidator grant 683083, RAMSES) for financial support.

Conflict of Interest

The authors declare no conflict of interest.

Keywords: coordination cages · dithienylethene · host-guest systems · photoswitches · supramolecular chemistry

[1] a) T. R. Cook, P. J. Stang, *Chem. Rev.* **2015**, *115*, 7001–7045; b) M. Han, D. M. Engelhard, G. H. Clever, *Chem. Soc. Rev.* **2014**, *43*, 1848–1860; c) G. Yu, K. Jie, F. Huang, *Chem. Rev.* **2015**, *115*, 7240–7303; d) H. Q. Peng, L. Y. Niu, Y. Z. Chen, L. Z. Wu, C. H. Tung, Q. Z. Yang, *Chem. Rev.* **2015**, *115*, 7502–7542; e) D. S. Kim, J. L. Sessler, *Chem. Soc. Rev.* **2015**, *44*, 532–546; f) D. Zhang, A. Martinez, J. P. Dutasta, *Chem. Rev.* **2017**, *117*, 4900–4942; g) S. Pullen, G. H. Clever, *Acc. Chem. Res.* **2018**, *51*, 3052–3064.

[2] a) T. Y. Kim, R. A. S. Vasdev, D. Preston, J. D. Crowley, *Chem. Eur. J.* **2018**, *24*, 14878–14890; b) G. Szaloki, V. Croue, V. Carre, F. Aubriet, O. Aleveque, E. Levillain, M. Allain, J. Arago, E. Orti, S. Goeb, M. Salle, *Angew. Chem. Int. Ed.* **2017**, *56*, 16272–16276; *Angew. Chem.* **2017**, *129*, 16490–16494; c) H. Wang, F. Liu, R. C. Helgeson, K. N. Houk, *Angew. Chem. Int. Ed.* **2013**, *52*, 655–659; *Angew. Chem.* **2013**, *125*, 683–687; d) D. Preston, P. E. Kruger, *Chem. Eur. J.* **2019**, DOI: 10.1002/chem.201805172.

[3] a) J. Li, D. Yim, W. D. Jang, J. Yoon, *Chem. Soc. Rev.* **2017**, *46*, 2437–2458; b) X. Su, I. Aprahamian, *Chem. Soc. Rev.* **2014**, *43*, 1963–1981; c) S. Uchiyama, E. Fukatsu, G. D. McClean, A. P. de Silva, *Angew. Chem. Int. Ed.* **2016**, *55*, 768–771; *Angew. Chem.* **2016**, *128*, 778–781; d) S. A. Rommel, D. Sorsche, S. Rau, *Dalton Trans.* **2016**, *45*, 74–77; e) A. Kumar, S.-S. Sun, A. J. Lees, *Coord. Chem. Rev.* **2008**, *252*, 922–939; f) X. Zhou, S. Lee, Z. Xu, J. Yoon, *Chem. Rev.* **2015**, *115*, 7944–8000; g) X. Sun, T. D. James, *Chem. Rev.* **2015**, *115*, 8001–8037; h) N. Busschaert, C. Caltagirone, W. Van Rossom, P. A. Gale, *Chem. Rev.* **2015**, *115*, 8038–8155.

[4] a) W. Q. Xu, Y. Z. Fan, H. P. Wang, J. Teng, Y. H. Li, C. X. Chen, D. Fenske, J. J. Jiang, C. Y. Su, *Chem. Eur. J.* **2017**, *23*, 3542–3547; b) S. K. Samanta, D. Moncelet, V. Briken, L. Isaacs, *J. Am. Chem. Soc.* **2016**, *138*, 14488–14496; c) A. Schmidt, V. Molano, M. Hollering, A. Pothig, A. Casini, F. E. Kuhn, *Chem. Eur. J.* **2016**, *22*, 2253–2256; d) W. Cullen, S. Turega, C. A. Hunter, M. D. Ward, *Chem. Sci.* **2015**, *6*, 625–631; e) B. Therrien, *Chem. Eur. J.* **2013**, *19*, 8378–8386; f) T. R. Cook, V. Vajpayee, M. H. Lee, P. J. Stang, K.-W. Chi, *Acc. Chem. Res.* **2013**, *46*, 2464–2474; g) J. E. M. Lewis, E. L. Gavey, S. A. Cameron, J. D. Crowley, *Chem. Sci.* **2012**, *3*, 778–784; h) D. Zhao, S. Tan, D. Yuan, W. Lu, Y. H. Rezenom, H. Jiang, L. Q. Wang, H. C. Zhou, *Adv. Mater.* **2011**, *23*, 90–93; i) X. Ma, Y. Zhao, *Chem. Rev.* **2015**, *115*, 7794–7839.

[5] D. B. Amabilino, D. K. Smith, J. W. Steed, *Chem. Soc. Rev.* **2017**, *46*, 2404–2420.

[6] a) S. Kassem, T. van Leeuwen, A. S. Lubbe, M. R. Wilson, B. L. Feringa, D. A. Leigh, *Chem. Soc. Rev.* **2017**, *46*, 2592–2621; b) H. Ube, Y. Yasuda, H. Sato, M. Shionoya, *Nat. Commun.* **2017**, *8*, 14296; c) C. Petermayer, H. Dube, *Acc. Chem. Res.* **2018**, *51*, 1153–1163.

[7] a) A. J. McConnell, C. S. Wood, P. P. Neelakandan, J. R. Nitschke, *Chem. Rev.* **2015**, *115*, 7729–7793; b) M. Xue, Y. Yang, X. Chi, X. Yan, F. Huang, *Chem. Rev.* **2015**, *115*, 7398–7501; c) X. Yan, F. Wang, B. Zheng, F. Huang, *Chem. Soc. Rev.* **2012**, *41*, 6042–6065; d) J. S. Park, J. L. Sessler, *Acc. Chem. Res.* **2018**, *51*, 2400–2410.

[8] a) Themed issue: Supramolecular Photochemistry, Ed. A. Credi, *Chem. Soc. Rev.* **2014**, *43*, 3995–4270; b) D. H. Qu, Q. C. Wang, Q. W. Zhang, X. Ma, H. Tian, *Chem. Rev.* **2015**, *115*, 7543–7588; c) T. Kakuta, T. A. Yamagishi, T. Ogoshi, *Acc. Chem. Res.* **2018**, *51*, 1656–1666.

[9] a) S. M. Jansze, G. Cecot, K. Severin, *Chem. Sci.* **2018**, *9*, 4253–4257; b) S. J. Wezenberg, B. L. Feringa, *Org. Lett.* **2017**, *19*, 324–327; c) J. Del Barrio, S. T. Ryan, P. G. Jambrina, E. Rosta, O. A. Scherman, *J. Am. Chem. Soc.* **2016**, *138*, 5745–5748; d) S. T. Ryan, J. Del Barrio, R. Suardiaz, D. F. Ryan, E. Rosta, O. A. Scherman, *Angew. Chem. Int. Ed.* **2016**, *55*, 16096–16100; *Angew. Chem.* **2016**, *128*, 16330–16334; e) T. Sakano, T. Ohashi, M. Yamanaka, K. Kobayashi, *Org. Biomol. Chem.* **2015**, *13*, 8359–8364; f) F. A. Arroyave, P. Ballester, *The J. Org. Chem.* **2015**, *80*, 10866–10873; g) J. Park, L. B. Sun, Y. P. Chen, Z. Perry, H. C. Zhou, *Angew. Chem. Int. Ed.* **2014**, *53*, 5842–5846; *Angew. Chem.* **2014**, *126*, 5952–5956; h) N. Kishi, M. Akita, M. Kamiya, S. Hayashi, H. F. Hsu, M. Yoshizawa, *J. Am. Chem. Soc.* **2013**, *135*, 12976–12979; i) M. Han, R. Michel, B. He, Y. S. Chen, D. Stalke, M. John, G. H. Clever, *Angew. Chem. Int. Ed.* **2013**, *52*, 1319–1323; *Angew. Chem.* **2013**, *125*, 1358–1362; j) G. H. Clever, S. Tashiro, M. Shionoya, *J. Am. Chem. Soc.* **2010**, *132*, 9973–9975.

[10] a) S. F. Pizzolato, B. S. L. Collins, T. van Leeuwen, B. L. Feringa, *Chem. Eur. J.* **2017**, *23*, 6174–6184; b) M. Vlatković, B. S. Collins, B. L. Feringa, *Chem. Eur. J.* **2016**, *22*, 17080–17111; c) T. Imahori, S. Kurihara, *Chem. Lett.* **2014**, *43*, 1524–1531; d) N. Vallavoju, J. Sivaguru, *Chem. Soc. Rev.* **2014**, *43*, 4084–4101; e) R. Göstl, A. Senf, S. Hecht, *Chem. Soc. Rev.* **2014**, *43*, 1982–1996; f) V. Blanco, D. A. Leigh, V. Marcos, *Chem. Soc. Rev.* **2015**, *44*, 5341–5370; g) R. S. Stoll, S. Hecht, *Angew. Chem. Int. Ed.* **2010**, *49*, 5054–5075; *Angew. Chem.* **2010**, *122*, 5176–5200.

[11] a) M. Han, Y. Luo, B. Damaschke, L. Gomez, X. Ribas, A. Jose, P. Peretzki, M. Seibt, G. H. Clever, *Angew. Chem. Int. Ed.* **2016**, *55*, 445–449; *Angew. Chem.* **2016**, *128*, 456–460; b) S. Chen, L. J. Chen, H. B. Yang, H. Tian, W. Zhu, *J. Am. Chem. Soc.* **2012**, *134*, 13596–13599; c) W. Wang, Y. X. Wang, H. B. Yang, *Chem. Soc. Rev.* **2016**, *45*, 2656–2693.

[12] a) C. D. Jones, J. W. Steed, *Chem. Soc. Rev.* **2016**, *45*, 6546–6596; b) S. C. Wei, M. Pan, Y. Z. Fan, H. Liu, J. Zhang, C. Y. Su, *Chem. Eur. J.* **2015**, *21*, 7418–7427; c) Y. Gu, E. A. Alt, H. Wang, X. Li, A. P. Willard, J. A. Johnson, *Nature* **2018**, *560*, 65–69.

[13] a) S.-Z. Pu, Q. Sun, C.-B. Fan, R.-J. Wang, G. Liu, *J. Mater. Chem. C* **2016**, *4*, 3075–3093; b) E. C. Harvey, B. L. Feringa, J. G. Vos, W. R. Browne, M. T. Pryce, *Coord. Chem. Rev.* **2015**, *282–283*, 77–86; c) M. F. Budyka, *Russ. Chem. Rev.* **2012**, *81*, 477–493; d) M. Irie, *Photochem. Photobiol. Sci.* **2010**, *9*, 1535–1542; e) R. Klajn, J. F. Stoddart, B. A. Grzybowski, *Chem. Soc. Rev.* **2010**, *39*, 2203–2237; f) C. Yun, J. You, J. Kim, J. Huh, E. Kim, *J. Photochem. Photobiol. C* **2009**, *10*, 111–129; g) K. Matsuda, M. Irie, *J. Photochem. Photobiol. C* **2004**, *5*, 169–182; h) H. Tian, S. Yang, *Chem. Soc. Rev.* **2004**, *33*, 85–97; i) M. Irie, *Chem. Rev.* **2000**, *100*, 1685–1716; j) M. Irie, T. Fukaminato, K. Matsuda, S. Kobatake, *Chem. Rev.* **2014**, *114*, 12174–12277; k) S. Kobatake, S. Takami, H. Muto, T. Ishikawa, M. Irie, *Nature* **2007**, *446*, 778–781; l) M. Morimoto, M. Irie, *J. Am. Chem. Soc.* **2010**, *132*, 14172–14178.

[14] a) D. J. van Dijken, J. M. Beierle, M. C. Stuart, W. Szymanski, W. R. Browne, B. L. Feringa, *Angew. Chem. Int. Ed.* **2014**, *53*, 5073–5077; *Angew. Chem.* **2014**, *126*, 5173–5177; b) K. Kawamura, K. Osawa, Y. Watanobe, Y. Saeki, N. Maruyama, Y. Yokoyama, *Chem. Commun.* **2017**, *53*, 3181–3184; c) T. C. Pace, V. Muller, S. Li, P. Lincoln, J. Andreasson, *Angew. Chem. Int. Ed.* **2013**, *52*, 4393–4396; *Angew. Chem.* **2013**, *125*, 4489–4492; d) T. Shiozawa, M. K. Hossain, T. Ubukata, Y. Yokoyama, *Chem. Commun.* **2010**, *46*, 4785–4787; e) K. Uchida, M. Walko, J. J. de Jong, S. Sukata, S. Kobatake, A. Meetsma, J. van Esch, B. L. Feringa, *Org. Biomol. Chem.* **2006**, *4*, 1002–1006; f) T. J. Wigglesworth, D. Sud, T. B. Norsten, V. S. Lekhi, N. R. Branda, *J. Am. Chem. Soc.* **2005**, *127*, 7272–7273; g) J. J. D. de Jong, L. N. Lucas, R. M. Kellogg, J. H. van Esch, B. L. Feringa, *Science.* **2004**, *304*, 278–281; h) S. Yamamoto, K. Matsuda, M. Irie, *Angew. Chem. Int. Ed.* **2003**, *42*, 1636–1639; *Angew. Chem.* **2003**, *115*, 1674–1677; i) E. Murguly, T. B. Norsten, N. R. Branda, *Angew. Chem. Int. Ed.* **2001**, *40*, 1752–1755; *Angew. Chem.* **2001**, *113*, 1802–1805; j) T. Kodani, K. Matsuda, T. Yamada, S. Kobatake, M. Irie, *J. Am. Chem. Soc.* **2000**, *122*, 9631–9637; k) T. Yamaguchi, K. Uchida, M. Irie, *J. Am. Chem. Soc.* **1997**, *119*, 6066–6071.

[15] C. Jenne, C. Kirsch, *Dalton Trans.* **2015**, *44*, 13119–13124.

[16] S. V. Ivanov, J. J. Rockwell, O. G. Polyakov, C. M. Gaudinski, O. P. Anderson, K. A. Solntsev, S. H. Strauss, *J. Am. Chem. Soc.* **1998**, *120*, 4224–4225.

[17] R. Li, J. J. Holstein, W. G. Hiller, J. Andréasson, G. H. Clever, *J. Am. Chem. Soc.* **2019**, DOI: 10.1021/jacs.8b1187.

Manuscript received: February 7, 2019
Revised manuscript received: March 20, 2019
Version of record online: April 16, 2019